Numerical Investigation of Unsteady Turbulent Flow of Incompressible Fluid around a Cylinder

M. Essahraoui[1], A. Ederouich[1] , R. El Bouayadi[1] and A. Saad[2]
[1](4) SEALAB, Systems Engineering Advanced Laboratory, Kenitra, Morocco
[2]National School of Applied Sciences, Ibn Tofail University, Kenitra, Morocco

Keywords: Turbulent, Unsteady Flow, Cylinder, Drag, Lift, FVM, $k-\varepsilon$.

Abstract: In this work we have investigated a numerical study of unsteady two-dimensional turbulent flow of incompressible fluid around and behind a cylinder with various diameter ($D_1 = 50mm,\ D_2 = 100mm$) $at\ R_e = 10\times10^3\ and\ R_e = 30\times10^3$, respectively. A numerical simulation will be used by CFD code to visualize the phenomenon of turbulent wakes generated behind a cylinder and the separation region around the surface cylinder. The standard $k-\varepsilon$ model is the numerical method used to manage the turbulent flow. This study led us to focus on the velocity contours, pressure contours, the static pressure distribution along the x-direction, the profiles of skin friction coefficients, and the variation of drag and lift coefficients as a function of time. The results obtained for the two cases considered gave us satisfactory results. The development of an oscillation region behind the cylinder, the variation of static pressure and skin friction coefficient along the cylinder, the mean velocity fields, pressure fields, all will be captured by the present simulation.

1 INTRODUCTION

The study of the characteristics flow of fluid around an object is essential for automotive, aeronautical and oil industries, but also for civil engineering. In particular, it is a prerequisite for the understanding of erosion phenomena in earthen dams, whether internal or external. The flow around or behind a cylinder is a classical fluid dynamics problem, and serves as a framework validating of new numerical methods. This academic problem has received a renewed interest during the last decade, both experimentally and numerically, due to the emergence of new methods for solving the equations of dynamics.

The studies have been done by the recent experiments demonstrated that the flow field is symmetrical upon the circular cylinder at values of $R_e \leq 5$, and as we increase the value of Reynolds number, the flow becomes unstable and the rate of mixing layers of fluid become more intense which causing the vortex shedding. (Dou, 2015)

Most of the experimental studies investigated the steady and unsteady behaviours of the alternating vortices in the wake. The work of (Tritton, 1971), (Lourenco & Shih, 1993), and (Braza, Chassaing, & Minh, 1990) should be mentioned. Besides these theoretical and numerical investigations, some experimental visualizations have been described by (Honji & Taneda , 1969), (Coutanceau & Defaye, 1991). (Rahman, Karim, & Alim, 2007)

The study of Hydrodynamic and aerodynamic phenomena of a wake modification behind an obstacle remains a fundamental problem in fluid dynamics fields. Thus, the vortex structures generate behind obstacles is of great interest in engineering practice. Indeed, the comprehension of the vortex structures produced behind these obstacles and their

different regimes are of primary use in constructing structures exposed to fluid flows. For a better visualization of the hydrodynamic and aerodynamic phenomena, a cylindrical obstacle is required because of their geometrical simplicity allowing numerical and experimental facilities. (Essel, Sharkey, & Tachine, 2014)

The objective of this numerical study, is to investigate the phenomena of unsteady two-dimensional turbulent flow of incompressible fluid around and behind a cylinder of diameter $D_1 = 50mm\ and\ D_2 = 100mm$ at $R_e = 10\times10^3\ and\ R_e = 30\times10^3$ respectively. Reynolds number based on the diameter of the cylinder, in our study we have focused to change the diameter of the

Essahraoui, M., Ederouich, A., El Bouayadi, R. and Saad, A.
Numerical Investigation of Unsteady Turbulent Flow of Incompressible Fluid around a Cylinder.
DOI: 10.5220/0010733200003101
In *Proceedings of the 2nd International Conference on Big Data, Modelling and Machine Learning (BML 2021)*, pages 311-315
ISBN: 978-989-758-559-3

cylinder and visualize how this change influence on the wake region behind the cylinder, and in the variation of drag, lift, static pressure, velocity profile and skin friction coefficient. Our work gives us a satisfactory result compared to the recent studies.

2 PHYSICAL MODEL

2.1 Mathematical Formulations

$$\frac{\partial u_i}{\partial x_i} = 0 \tag{1}$$

$$\frac{\partial u_i}{\partial t} + u_j \frac{\partial u_i}{\partial x_j} = -\frac{1}{\rho}\frac{\partial p}{\partial x_i} + \nu \frac{\partial^2 u_i}{\partial x_j^2} - \frac{\partial \overline{u_i' u_j'}}{\partial x_j} \tag{2}$$

$$\overline{-\partial u_i' u_j'} = \nu_T \left(\frac{\partial u_i}{\partial x_j} + \frac{\partial u_j}{\partial x_i}\right) - \frac{2}{3} k \delta_{ij} \tag{3}$$

$$\frac{\partial \rho k}{\partial t} + \frac{\partial \rho k u_i}{\partial x_i} = \frac{\partial}{\partial x_j}\left[\left(\mu + \frac{\mu_T}{\sigma_k}\right)\frac{\partial k}{\partial x_j}\right] + G_k - \rho\varepsilon \tag{4}$$

$$\frac{\partial \rho \varepsilon}{\partial t} + \frac{\partial \rho \varepsilon u_i}{\partial x_i} = \frac{\partial}{\partial x_j}\left[\left(\mu + \frac{\mu_T}{\sigma_\varepsilon}\right)\frac{\partial \varepsilon}{\partial x_j}\right] + C_{1\varepsilon}\frac{\varepsilon}{k}(G_k) - C_{2\varepsilon}\rho\frac{\varepsilon^2}{k} \tag{5}$$

Where $i, j = 1,2$

$$\begin{cases} x_1: horizontal\ direction \\ x_2: vertical\ direction \end{cases}$$

u_1, u_2: *mean velocity components*

$\overline{u_i' u_j'}$: *Reynolds stress components*

$u_{i,j}'$: *Fluctuating part of the velocity*

p: *Dynamic pressure*

ρ: *The density of the fluid*

k: *The turbulent kinetic energy*

ε: *The dissipation rate*

ν_T: *Turbulent viscocity*

G_k: *Generation of turbulence kinetic energy*

$C_{1\varepsilon}, C_{2\varepsilon}$: *Empirical coefficients of* $k - \varepsilon$

$\sigma_k, \sigma_\varepsilon$: *Turbulent prandtl number for* k *and* ε

For our study, we have chosen the standard $k - \varepsilon$ model, so the values of empirical coefficients are:

$$C_{1\varepsilon} = 1.44, C_{2\varepsilon} = 1.92, \sigma_k = 1.0, \sigma_\varepsilon = 1.3, C_\mu = 0.09$$

The governing equations have been discretized by the finite volume method (FVM). The SIMPLE scheme algorithm has been used by the coupling of pressure, and velocity. The Reynolds numbers values are depended on the variation of the cylinder diameter. (Kaur & Kumar, 2018)

2.2 Geometric and Meshing

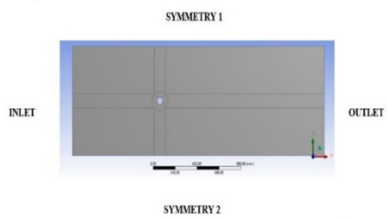

Figure 1: The computational Domain.

The computational domain is a surface of dimension 800x2300. The diameter of each cylinder is ($D_1 = 50mm\ and\ D_2 = 100mm$) .The upstream length is 800mm and the downstream length is 1500mm from the centre of the cylinder.

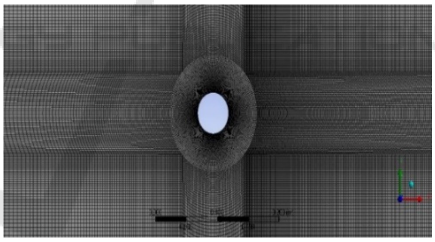

Figure 2: The grid around the cylinder.

A fine refined mesh around the cylinder is required to have better accuracy of the results by the CFD solver, and the method used for our mesh is the **Rectangular domain with smooth quadrilateral grids.** (Salehi, Mazaheri, & Kazeminezhad, 2018)

2.3 Characteristic Parameter

Drag and lift coefficients are the fundamental characteristics parameters for better understanding the motion of fluid around a cylinder. (Shim, Sharma, & Richards, 2009) The Strouhal number is describing the oscillating flow mechanism in order to study vortex shedding. The pressure coefficient is a dimensionless term, which describes the relative pressure through the flow field. Moreover, the skin friction coefficient dimensionless parameter describes the aerodynamic resistance due to the contact of moving fluid on the surface of the cylinder. All these parameters are defined as follows:

$$C_d = \frac{2F_d}{\rho V_\infty^2 A} \quad (6)$$

$$C_l = \frac{2F_l}{\rho V_\infty^2 A} \quad (7)$$

$$C_f = \frac{\tau_w}{\frac{1}{2}\rho V_\infty^2} \quad (8)$$

$$C_P = \frac{P - P_\infty}{\frac{1}{2}\rho V_\infty^2} \quad (9)$$

$$S_t = \frac{fL}{V_\infty} \quad (10)$$

$\boldsymbol{A}$: $Projected\ Area$
$\boldsymbol{f}$: $The\ frequency\ of\ vortex\ sheeding$
$\boldsymbol{L}$: $The\ characteristic\ length\ i.e\ cylinder\ diameter$
$\boldsymbol{\tau_w}$: $Skin\ shear\ stress\ on\ a\ cylinder\ surface$
$\boldsymbol{P}$: $The\ static\ pressure\ at\ the\ point\ at\ which\ pressure\ coefficient\ has\ been\ evaluated.$
$\boldsymbol{P_\infty}$: $The\ static\ pressure\ in\ the\ free\ stream.$
$\boldsymbol{F_d}, \boldsymbol{F_l}$: $Drag\ and\ Lift\ force\ respectively$

3 RESULTS

Since we are studying the effect of fluid flow on two various cylinder diameter with an unsteady turbulent incompressible flow, the velocity and pressure contours do not manifest a sizeable difference with the literature, and it can be notice that there are big vortices that develop downstream of the cylinder whose they are ejected in alternation sometimes towards the upper and the lower wall. See figures 3, 4, 5 and 6. The velocity and pressure profiles around the cylinder ($\boldsymbol{D_1 = 50mm\ and\ D_2 = 100mm}$) at different x positions have been visualized by the present simulation. See figures 7 and 8. The drag and lift coefficients around the cylinder vary with time in the form of quasi sinusoidal curve. See figures 9 and 10. The skin friction coefficient increases relatively linearly from the stagnation point $\mathbf{x = -0.05\ (D_2 = 100mm)\ and\ x = -0.025\ (D_1 = 50mm)}$, until it reaches a maximum level at approximately $\mathbf{-0.035 \le x \le -0.015}$ at different Reynolds number values. This location is upstream of the cylinder, approximately 0,35≤$\boldsymbol{Cf}$≤0,045, as we will observe in the figures below, and then it gradually decreases before stabilizing to an asymptotic value. See figure 11.

3.1 Velocity Contours

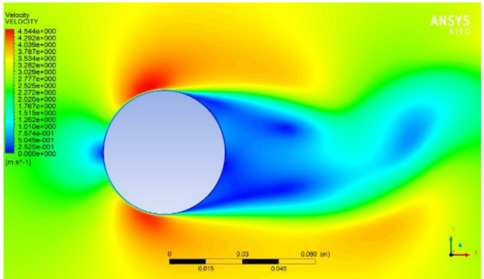

Figure 3: Velocity contours at $R_e = 10 \times 10^3$.

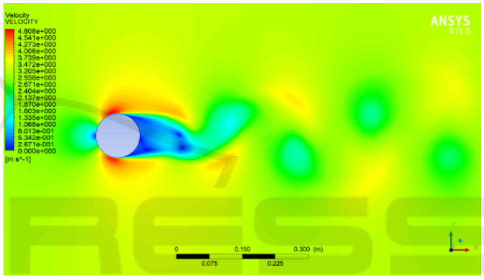

Figure 4: Velocity contours at $R_e = 30 \times 10^3$.

3.2 Pressure Contours

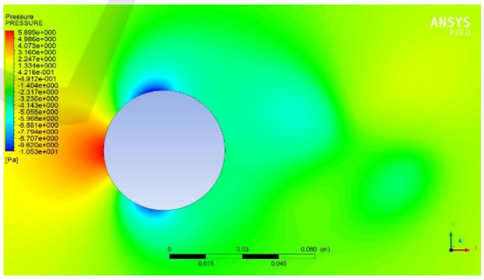

Figure 5: Pressure contours at $R_e = 10 \times 10^3$.

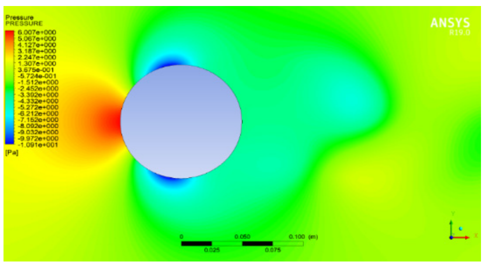

Figure 6: Pressure contours at $R_e = 30 \times 10^3$.

3.3 Velocity Profiles

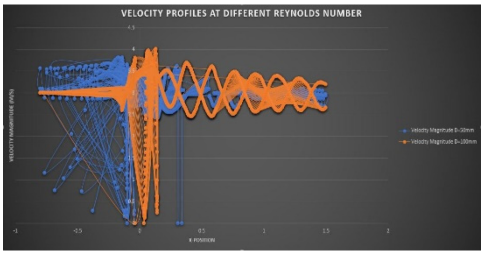

Figure 7: Velocity profiles x=±1.5 at different Reynolds number.

3.4 Pressure Profiles

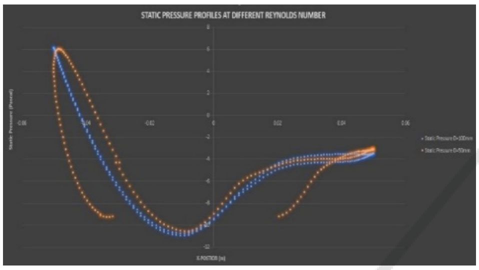

Figure 8: Pressure Profiles X=±0.06 at Different Reynolds NUMBER.

3.5 Drag & Lift Coefficient at $R_e = 10 \times 10^3$

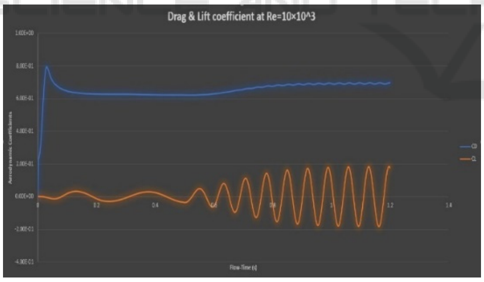

Figure 9: Variation of the coefficient of drag and lift in the case of D=50MM.

3.6 Drag and Lift Coefficient at $R_e = 30 \times 10^3$

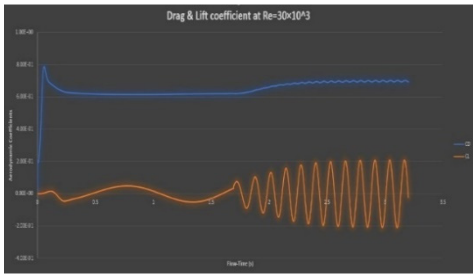

Figure 10: Variation of the coefficient of drag and lift in the case of D=100mm.

3.7 Skin Friction Coefficient

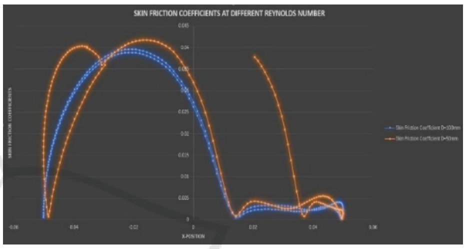

Figure 11: Variation of Skin friction coefficient at different R_e.

4 CONCLUSIONS

The study of unsteady 2D turbulent flow around obstacles was the objective of the present work. Numerical simulation has been adopted by resolve the equations of an unsteady flow of an incompressible fluid of a turbulent regime. We compared our results with those obtained in the literature for a flow around a cylinder. We have visualized the phenomenon of vortex shedding, which has been generated by unfavorable pressure gradient at the separation points on the cylinder surface. Thus, the pressure values are lower above and below the cylinder and an oscillation region behind the cylinder was observed for both Reynolds number. In the middle of the vortex area, the velocity and pressure are low compared to the extremity. The variation of the lift and drag coefficients are simultaneous with the vortex shedding detachment. This detachment is responsible for the creation of large vortices behind the cylinder. We can notice from the graphs of static pressure and skin friction coefficient that the values of pressure and skin friction coefficient are not identical around the cylinder, and the flow is separated on the cylinder surface.

REFERENCES

Braza, M., Chassaing, P., & Minh, H. H. (1990). Prediction of Large-Scale Transition features in the wake. *Phys. Fluids, A2*(8), 1461-1471.

Coutanceau, M., & Defaye, J. R. (1991). Circular Cylinder Wake Configurations- A flow Visualization. *44*(6).

Dou, H.-S. (2015, March). Simulation and Instability Investigation of the Flow around a Cylinder between Two Parallel Walls. *Journal of Thermal Science, 24*(2), 140-148.

Essel, E. E., Sharkey, L., & Tachine, M. F. (2014, August). Effects of gap ratio on flow past a square cylinder. *In Fluids Engineering Division Summer Meeting*.

Honji, H., & Taneda , S. (1969). Unsteady Flow Past a Circular Cylinder. *J. Phys*, 1668-1677.

Kaur, M., & Kumar, P. (2018, August). Numerical investigation of flow over a circular cylinder at different gap ratios. *In IOP Conference Series: Materials Science and Engineering, Vol.402*(No.1).

Lourenco, L. M., & Shih, C. (1993). Characteristics of the Plane Turbulent Near Wake of a Circular. *A Particle Image Velocimetry Study, Private Communication*.

Rahman, M., Karim, M., & Alim, A. (2007). Numerical investigation of unsteady flow past a circular cylinder using 2-D finite volume method. *Journal of Naval Architecture and Marine Engineering, 4*(1), 27-42.

Salehi, M. A., Mazaheri, S., & Kazeminezhad, M. H. (2018). Study of Flow Characteristics Around a Near-Wall Circulair Cylinder Subjected to a Steady Cross-Flow. *International journal of coastal & offshore engineering, 1*(4), 45-55.

Shim, Y. M., Sharma, R. N., & Richards, P. J. (2009, June). Numerical study of the flow over a circular cylinder in the near wake at Reynolds number 3900. *In 39th AIAA Fluid Dynamics Conference (p. 4160)*.

Tritton, D. J. (1971). A Note on Vortex Streets behind Circular Cylinders. *J. Fluid Mech, 45*(203).